ACADEMIC
PRESS

High-sensitivity sapphire cells for high pressure NMR spectroscopy on proteins

Martin Reinhard Arnold, Hans Robert Kalbitzer, and Werner Kremer*

Institut für Biophysik und physikalische Biochemie, Universität Regensburg, D-93040 Regensburg, Germany

Abstract

High pressure NMR spectroscopy is a most exciting method for studying the structural anisotropy and conformational dynamics of proteins. The restricted volume of the high pressure glass cells causes a poor signal to noise ratio which up to now renders the application of most of the multidimensional NMR experiments impossible. The method presented here using high strength single crystal sapphire cells doubles the signal-to-noise ratio and allows to perform high pressure NMR measurements more easily. As a first application the difference of partial molar volumes caused by *cis–trans*-isomerisation of a prolyl peptide bond in the tetrapeptide Gly-Gly-Pro-Ala could be determined as $0.25\,\mathrm{ml\,mol^{-1}}$ at 305 K.
© 2003 Elsevier Science (USA). All rights reserved.

1. Introduction

High pressure NMR-spectroscopy can give a wealth of important information about protein biochemistry and biophysics at atomic resolution which cannot or can only be obtained very difficult by other methods (for a review see [1,2]). It can give information about mechanical and dynamical properties of proteins and can be used to stabilise folding and unfolding intermediates. When pressures of 200 MPa are applied it allows the observation of protein denaturation at temperatures down to 255 K. In addition protein aggregation and association can be influenced by pressure [3].

Two conceptually different methods are at present applied for high pressure NMR experiments: the first method uses specifically designed non-magnetic metal autoclaves [4,5]. The second method is the so called Yamada glass cell method [6–8]. Although in principle pressurising of the whole probe head appears to be the superior method since very high pressures can be obtained, the design of special metallic high pressure probe heads leads to severe problems. These are mainly due to the limited space in high resolution high field NMR spectrometers, perturbations of the magnetic field homogeneity and the difficulty to construct reliable low impedance radiofrequency feedthroughs through the thick metal parts of the autoclaves. Especially the latter difficulties increase with increasing RF frequency. The Yamada glass cell method can be applied much easier since it does not require special probe heads. The main disadvantage of the glass cell method is the inherent low sensitivity since the sample volume contained in the thick-walled sample tubes is rather small. Typically, borosilicate or quartz glass capillaries with an outer diameter of 5 mm and an inner diameter of 1.0–1.2 mm are required to withstand a pressure up to 200 MPa. A few of these capillaries can be used up to a pressure of 400 MPa, a pressure which can be reached routineously with capillaries with an outer diameter of 1 mm [9,10].

The typical active volume in 5 mm capillaries is 40 μL, that of the 1 mm capillaries is 0.3 μL. The small amount of sample material within the NMR-coils causes a too poor signal-to-noise ratio for useful applications of most of the multidimensional NMR experiments important in protein science. Therefore, set ups with larger active volumes are needed. The maximum pressure $p_{\max}$

---

* Corresponding author. Fax: +49-941-9432479.

E-mail address: werner.kremer@biologie.uni-regensburg.de (W. Kremer).

obtainable is a function of the tensile strength τ of the material and the quotient of the outer and inner diameters d_o and d_i. It can be approximated by

$$p_{max} = \tau \ln(d_o^2/d_i^2). \tag{1}$$

In Table 1 mechanical and physical parameters of different materials used for the production of high pressure capillaries are listed. The tensile strength of borosilicate glass is much lower than that of quartz and sapphire. The effective tensile strength given in Table 1 includes the possible existence of faults in the material. The occurrence of faults substantially reduces the maximum pressure the capillaries can withstand, their number is also much dependent on the details of fabrication process. As the probability for faults decreases with size of the piece of material, small capillaries can withstand much higher forces. The quartz cells tested in our laboratory generally failed in reaching higher pressures than the borosilicate capillaries, in spite of their seven times higher tensile strength of quartz. However, selected quartz capillaries with an outer diameter of 3 mm and an inner diameter of 1 mm were reported to withstand pressures up to 400 MPa [11–13]. Yamada reported, that quartz capillaries made out of synthetic quartz can withstand pressures up to 600 MPa [8]. Even borosilicate glass capillaries can be used up to 400 MPa but the outer diameter is only 1 mm and the inner diameter 0.1 mm [9,10].

The use of sapphire cells with 5 mm outer diameter and 0.8 mm wall was first suggested by Roe [14] for pressures up to 41.5 MPa. Urbauer et al. [15] reported, that sapphire cells with 5 mm outer diameter and 1 mm inner diameter withstand pressures up to 100 MPa (US patent #5977772).

Single crystalline sapphire cells with an inner diameter of 1.73 mm and an outer diameter of 3.18 mm are available from Saphikon (Milford, New Hampshire 03055, USA). In contrast to amorphous materials such as borosilicate and quartz glass, in general sapphire single crystal should contain only few faults due to the manufacturing method. However, the commercially available sapphire cells have still a large spread in their quality and have to be tested before use. Although most cells can be used up to 200 MPa, some of them burst at

pressures below 70 MPa but also pressures above 350 MPa were reached. A disadvantage of sapphire relatively to borosilicate glass is its relatively high thermal expansion coefficient which may lead to mechanical problems when changing the temperature.

In general, the sapphire cells can be used with a structure according to the descriptions of Price and Lüdemann [7] for borosilicate glass cells. Here, the pressurising fluid (methyl cyclohexane:methyl cyclopentane/50:50) is pressurised externally by a pressure bench which is connected to the autoclave by a 6 m high strength steel tube with an inner diameter of 100 μm. The pressure is transmitted onto the NMR-sample by a Teflon hose closed by a Teflon plug which simultaneously serves as separation of the organic solvent from the biological sample (Fig. 1). For sealing the glass cell system cone shaped nipples are used. These nipples are tightly pressed into the cone shaped bore of the autoclave. Since the radial forces applied to the capillary tube increase with its diameter, only small diameters in the contact area of the capillary with the sealing cone can be used. This does not present a problem for glass cell systems because the glass cells can be shaped appropriately in this region. Since the outer diameter of the sapphire capillary is constant over its length another type of pressure sealing had to be devised for the sapphire cells. To fix the capillaries within the autoclave a 30 mm long cylinder shaped TiAl6V4 nipple was used which was glued around the end of the capillary. The small gap between bore of the autoclave and nipple (<10 μm) is sealed by an O-ring. The O-ring is forced to the walls of the autoclave by a cone shaped brass cylinder. A glass rod is used to fill up the inner volume of the sapphire cell outside the NMR coil, to reduce the amount of sample fluid needed to fill the sample tube. To prevent the probe head from damages caused by an explosion a Teflon burst protection is applied to the lower end of the capillaries (Fig. 1).

2. Results

To show the improvements achieved by using the new sapphire cells ^{1}H–^{15}N-HSQC experiments were per-

Table 1
Physical and mechanical properties of the materials used for high pressure NMR capillaries[a]

	Borosilicate glass	Quartz glass	Sapphire	
Producer	Schott	Qsil		Saphikon
Tensile strength [Nm m^{-2}]	7	50		140
Coeff. of expansion [10^{-6} K^{-1}]	3	0.5	8.8	7.9
Temp. of processing [K]	825–1260	1700–2100		>2053
Magn. susceptibility [10^{-9} m^3 kg^{-1}]	−0.86	−0.49	−0.21	−0.25

[a] The data are taken from the datasheets of the manufacturers [22–24], the magnetic susceptibilities of borosilicate and quartz glass were taken from Wilmad [25] and Lide [26], respectively. Due to its single crystalline structure, the coefficient of expansion and magnetic susceptibility of sapphire are tensorial quantities (the left side, values parallel, right side perpendicular to the principal axis of the system).
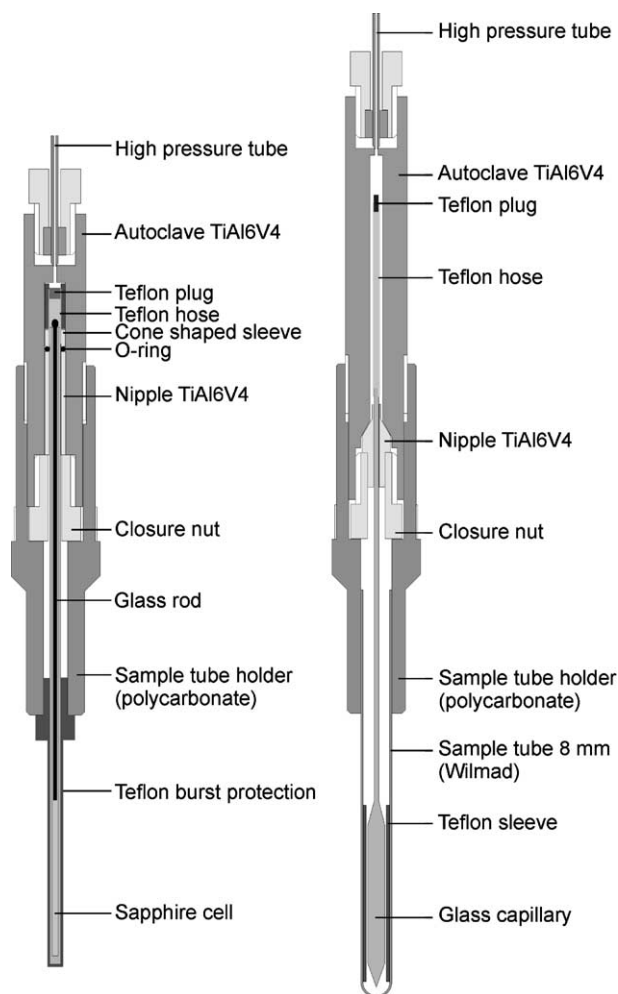
Fig. 1. Borosilicate glass and sapphire high pressure systems. (Left) Sapphire cell system with O-ring gasket. The pressurising fluid and sample are separated by a Teflon shrink hose, which is closed by a Teflon plug. Outer diameter of the sapphire cell 3.18 mm, inner diameter 1.73 mm. As burst protection either a Teflon hose with 0.2 mm wall thickness or a especially manufactured closed Teflon tube (outer diameter 4.8 mm, inner diameter 3.5 mm) was used. (Right) Glass cell system with cone shaped metal sealing. The Duran 50 borosilicate glass capillary is glued into a cone shaped TiAl6V4 nipple. Outer diameter of the glass capillary 5.0 mm, inner diameter 1.2 mm.

formed with a sample of a 0.5 mM sample of the cold shock protein (Csp) from *Thermotoga maritima*. The sample was measured in the sapphire cell with an outer diameter of 3.18 mm and an inner diameter of 1.73 mm and then under identical experimental conditions in the glass cell with 5 mm outer diameter and 1.2 mm inner diameter. A part of the spectra measured with this equipment are shown in Fig. 2. The data were plotted at the same contour level. It is obvious that the signal-to-noise ratio is much better using the sapphire cell as to be expected from the approximately two-times larger active volume in the probe head. 1D traces through the maximum of the H^N crosspeaks of K19 in the 2D HSQC spectra are depicted in the bottom part of Fig. 2. The

signal-to-noise ratio calculated from 1D-traces is increased by a factor of 2, in line with the expectation. Since the glass cell together with their safety Teflon tubes does not fit in a 5 mm probe head, the 3 mm sapphire cell could also be used in a 5 mm probe head leading to a further improvement in signal-to-noise ratio.

A first result of the sapphire cells which could not be obtained before with the glass cell method is presented in Fig. 3. The peptide bonds in proteins are known to be almost always in *trans*-configuration, only for peptide bonds involving the imino group of a proline a significant probability for the *cis*-configuration exists. The exchange between both conformations is slow on the NMR-timescale and therefore can be observed easily by NMR-spectroscopy. In protein folding, the *cis–trans*-isomerisation can be a time-limiting process and is enhanced by prolyl peptidyl isomerases *in vivo*.

Both isomers of the proline peptide bond can be distinguished by the different chemical shift values of the prolyl signals in the NMR spectra. For our experiments we used a 5 mM solution of the random-coil peptide GGPA (glycyl-gycyl-prolyl-alanine). In a recent study we could not find a significant pressure dependence of the *cis–trans*-equilibrium using a glass-cell [16] at the actual experimental error. This result was in line to previous reports [17–19] which have stated that conformational equilibria in small molecules are affected by pressure only if it changes local electrical charges of the concerned conformational states. Examples are *N*-acetyl-L-proline-NH-methylamide and glycylsarcosine [20].

The increased signal-to-noise of the sapphire cell allowed a reinvestigation of this phenomenon (Fig. 3). The conformational equilibrium of the prolyl peptide bond was studied by integrating the H^α-signals of *cis*- and *trans*-isomer of proline which are well separated in the 1D-spectra. Integration of the line volume gives the population of the corresponding isomer. As a result now a significant shift of the equilibrium constant $K = [trans]/[cis]$ can be observed when the pressure is varied. At 0.1 MPa and 305 K the value of K is 3.381 ± 0.008. Increasing pressure leads to a higher population of the *cis*-isomer of the peptide bond. From the dependence of K on the pressure p the change of the partial molar volume ΔV^0 can be calculated as $-0.25 \, \text{ml mol}^{-1}$ at 305 K for the transition from the *trans*-configuration to the *cis*-configuration. A possible explanation for the effect found is the breakage of two H-bonds which are forming γ-turns [21] in the short peptide GGPA between the carboxyl C and the amide N of the C-terminal alanine and the second glycine but may also represent differences of the partial charges of the peptide bond itself in the two isomers.

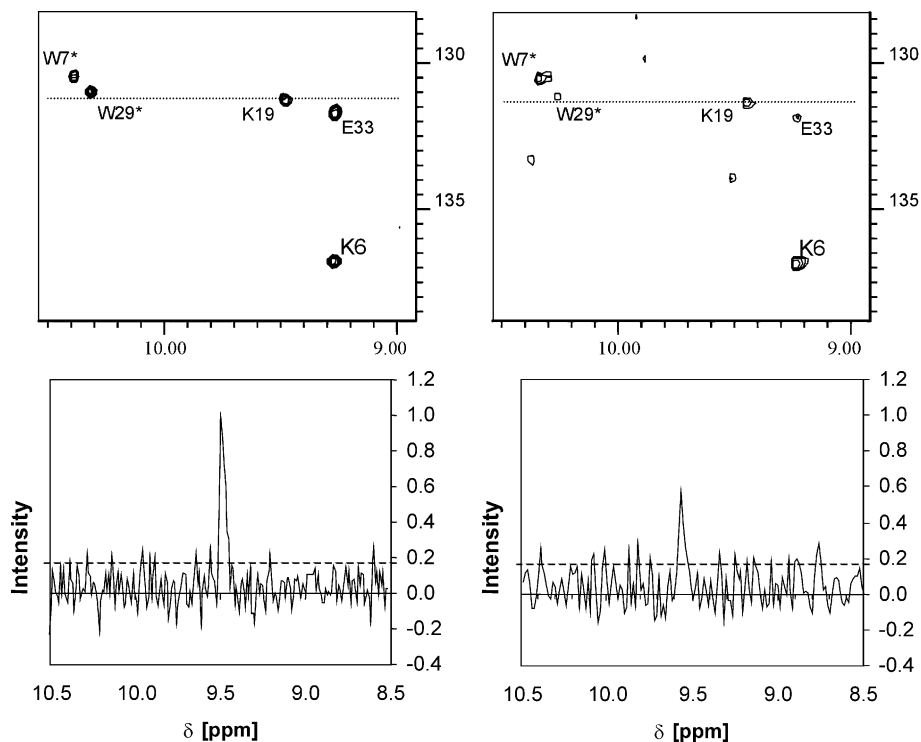In conclusion, the newly developed sapphire cell system allows a detection of pressure effects in

Fig. 2. Sensitivity obtainable in high pressure borosilicate glass cells and sapphire cells. The sample contained 0.5 mM uniformly ^{15}N-enriched cold shock protein from *T. maritima* (*Tm*Csp) in 50 mM phosphate buffer (pH 6.5), 20 mM NaCl, 0.2 mM Na–EDTA, 0.1 μM NaN$_3$, 10% D$_2$O, and 90% [1]H$_2$O. Gradient selected sensitivity enhanced ^{1}H –^{15}N-HSQC spectra were recorded under identical experimental conditions either in a sapphire cell (left) with an outer diameter 3.18 mm, inner diameter 1.73 mm or a borosilicate glass capillary (right) with an outer diameter of 5.0 mm and an inner diameter of 1.2 mm. Data were recorded with a 8 mm inverse triple resonance probe head at 600 MHz proton frequency. Total acquisition time approximately 2.5 h, resolution 2048 points in the direct dimension and 256 points in the indirect dimension. The temperature was adjusted to 303 K. (Top) Only a small part of the spectra are shown and plotted at the same contour levels for the two experiments. (Bottom) 1D-trace through the maximum of the H^N-signal of K19.
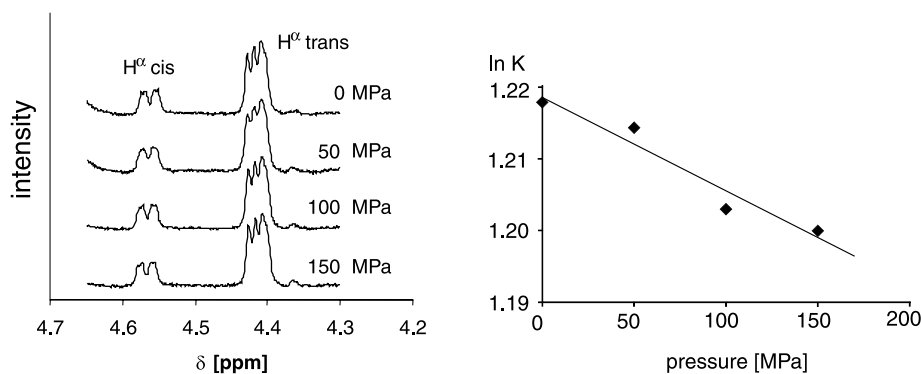

Fig. 3. Left: 1D-^{1}H spectra of the H$^\alpha$ protons of proline in the tetrapeptide GGPA. The sample contained 5 mM GGPA in 50 mM Tris/HCl buffer (pH 7.0) and 0.1 mM DSS in 99% D$_2$O. (Left) Part of 1D ^{1}H-NMR spectra at various pressures showing the H$^\alpha$-signal of proline in *cis*- and *trans*-conformation, respectively. The pressure was changed from 0.1 to 150 MPa in steps of 50 MPa at a temperature of 305 K. (Right) The logarithm of the equilibrium constant K (the ratio of the integrals of the signals of the *trans*- to the *cis*-conformer) is plotted as function of pressure p. The change of partial molar volume ΔV^0 is obtained from equation $\ln K = -1/RT(\Delta G^0 + p\Delta V^0)$.

peptides and proteins with a much higher sensitivity than that obtained in conventional systems and should allow the performance of multidimensional spectroscopy at high pressure which was not possible before.

References

[1] K. Akasaka, H. Li, H. Yamada, R. Li, T. Thoresen, C.K. Woodward, Pressure response of protein backbone structure. Pressure-induced amide ^{15}N chemical shifts in BPTI, Protein Sci. 8 (1999) 1946–1953.

[2] K. Akasaka, H. Yamada, On-line cell high-pressure nuclear magnetic resonance technique: application to protein studies, Methods Enzymol. 338 (2001) 134–158.

[3] M. Gross, R. Jaenicke, Proteins under pressure. The influence of high hydrostatic pressure on structure function and assembly of proteins and protein complexes, Eur. J. Biochem. 221 (2) (1994) 617–630.

[4] F. Bachl, NMR-Spektroskopische Untersuchungen zur Dynamik einfacher Kohlenwasserstoffe bis 600 MPa, Dissertation, Universität Regensburg, 1988.

[5] L. Ballard, A. Yu, C. Reiner, J. Jonas, A high pressure high-resolution NMR probe for experiments at 500 MHz, J. Magn. Res 133 (1998) 190–193.

[6] H. Yamada, Pressure-resisting glass cell for high pressure, high-resolution NMR measurements, Rev. Sci. Instr. 45 (1974) 540–542.

[7] W.E. Price, H.-D. Lüdemann, NMR and diaphragm cell techniques for the study of molecular dynamics in fluids, in: W.B. Holzapfel, N.S. Isaacs (Eds.), High Pressure Techniques in Chemistry and Physics: A Practical Approach, Oxford University Press, Oxford, 1997, p. 225, Chapter 5.

[8] H. Yamada, K. Nishikawa, M. Honda, T. Shimura, K. Aksaka, K. Tabayashi, Pressure-resisting cell for high-pressure, high-resolution nuclear magnetic resonance measurement at very high magnetic fields, Rev. Sci. Instr. 72 (2001) 1463–1471.

[9] F.X. Prielmeier, E.W. Lang, R.J. Speedy, H.-D. Lüdemann, The pressure dependence of self diffusion in supercooled light and heavy water, Ber. Bunsenges. Phys. Chem. 92 (1988) 1111.

[10] M.R. Arnold, H.-D. Lüdemann, The pressure dependence of self diffusion and spin lattice relaxation in cold and supercooled H_2O and D_2O, Phys. Chem. Chem. Phys. 4 (2002) 1581–1586.

[11] K. Akasaka, H. Li, P. Dubovskii, H.R. Kalbitzer, H. Yamada, High resolution-high pressure NMR spectroscopy: application to protein structure dynamics and folding, in: O. Jardetzky, M.D. Finucane (Eds.), Dynamics Structure and Function of Biological Macromolecules, IOS Press, 2001, pp. 77–92.

[12] N. Karger, H.-D. Lüdemann, M.G. Sceats, Pressure dependence of the OH-stretch Raman spectra of supercooled water, Ber. Bunsenges. Phys. Chem. 99 (1995) 1104.

[13] N. Karger, M.G. Sceats, H.-D. Lüdemann, Raman spectroscopy of supercooled water at high pressures, in: H.J. White, J.V. Sengers, D.B. Neumann, J.C. Bellows (Eds.), Physical Chemistry of Aqueous Systems. Proceedings of the 12th International Conference on the Properties of Water and Steam, Begell House, New York, 1995, p. 386.

[14] D.R. Roe, Sapphire NMR tube for high-resolution studies at elevated pressures, J. Magn. Res. 63 (1985) 388–391.

[15] J.L. Urbauer, M.R. Ehrhardt, R.J. Bieber, P.F. Flynn, A.J. Wand, High resolution triple-resonance NMR spectroscopy of a novel calmodulin peptide complex at kilobar pressures, J. Am. Chem. Soc. 118 (1996) 11329–11330.

[16] M.R. Arnold, W. Kremer, H.-D. Lüdemann, H.R. Kalbitzer, ^{1}H-NMR parameters of common amino acid residues measured in aqueous solutions of the linear tetrapeptides Gly-Gly-X-Ala at pressures between 0.1 and 200 MPa, J. Phys. Biochem 96 (2002) 129–140.

[17] A. Drljaca, C.D. Hubbard, R. van Eldik, T. Asano, M.V. Basilevski, W.J. le Noble, Activation and reaction volumes in solutions, Chem. Rev. 98 (1998) 2167–2284.

[18] J. Hauer, G. Völkel, H.-D. Lüdemann, High-pressure high-resolution nuclear magnetic resonance. Part IV ΔV^+ and ΔG^+ for the rotation of the amide group in formamide, acetamide, *N,N*-diethylbenzamide, *N,N*-di-isopropylbenzamide and *N*-isopropyl-*N*-methylacetamide, J. Chem. Res. (S) (1980) 16–17.

[19] G. Klimke, J. Hauer, H.-D. Lüdemann, W. Pfleiderer, The activation volume of the *syn* ⟺ *anti* rotation of lumazine β-riboside, J. Chem. Res. (S) (1981) 80–81.

[20] H. Hauer, H.-D. Lüdemann, R. Jaenicke, Free activation energies and activation volumes for the amide rotation in some peptides studied by high pressure ^{1}H-high resolution NMR, Z. Naturforsch. C 37 (1982) 51–56.

[21] G. Némethy, M.P. Printz, The γ-turn, a possible folded conformation of the polypeptide chain. Comparison with the β-turn, Macromolecules 5 (1972) 755–758.

[22] Schott-Rohrglas GmbH, DURAN Glas Katalog 2000, Röhren, Kapillaren und Stäbe aus Borosilicatglas 3.3, p. 12–13 (2000).

[23] QSIL Katalog Quarzschmelze Ilmenau GmbH, Laborgeräte und Sondererzeugnisse aus Quarzglas, p. 5 (1997).

[24] Saphikon, Properties and Benefits of Sapphire: A Quick Reference Guide, (2001) http://www.saphikon.com/qrg.pdf.

[25] Wilmad, Services and Information, NMR-002: Sample Devices and Magnetic Susceptibility (1998), http://www.wilmad.com/NMR002.html.

[26] D. Lide, CRC Handbook of Chemistry and Physics, 81st Ed., (2000–2001).